

Probe Techniques for Low-Density Plasmas

Francis F. Chen

Plasma Physics Laboratory, Princeton University, Princeton, N. J.

I. INTRODUCTION

The use of electrostatic probes in thermally ionized cesium and potassium plasmas requires some rather special techniques because of the extremely low densities and temperatures which are encountered. Among the problems encountered in measuring the dc properties of the plasma are 1) the change of work function of the probe surface; 2) the loss of plasma on the probe by recombination; 3) the inadequacy of probe theory for $r_p \approx \lambda_D$, where r_p is the probe radius and λ_D the Debye length; and 4) the high levels of impedance necessary to "float" a probe system. When a probe is used for measurement of fluctuations, two further problems arise: 1) adequate shielding of the probe, and 2) the frequency response of the probe and its circuitry. This paper is devoted to the problem of frequency response.

The first requirement for a probe is that it should not disturb the plasma; in strong magnetic fields this amounts to the condition $r_s \ll r_{Li}$, where r_{Li} is the ion gyroradius and r_s is the overall radius of the probe. Since $r_p < r_s$, this requires the use of small probe tips and hence implies small probe currents. A second requirement is that the frequency response be good to the ion gyrofrequency

f_{ci} , which is about 200 kHz for potassium at 5 kG. This range includes all low-frequency phenomena such as drift waves, acoustic waves, cyclotron waves, and drift-cyclotron waves but of course does not cover high-frequency phenomena such as electron or hybrid oscillations. (The latter can be detected by probes, but not Langmuir probes.) Since the probe sheath can be expected to respond to frequencies below the ion plasma frequency ω_{pi} , the frequency response of the sheath is no problem if $\omega_{pi} \gg \omega_{ci}$, which is almost always the case. The goal we have set for frequency response is particularly hard to satisfy for floating potential measurements, but it is important that \tilde{V}_f be measured without phase shift because the anomalous transport of plasma across the magnetic field can be shown to be proportional to $B^{-1} \langle \tilde{n} \tilde{E}_\theta \rangle$, and this can be determined directly by correlation measurements between \tilde{n} and \tilde{V}_f .

Consider the diagram of Fig. 1, which is typical of what is used to observe oscillations. Let C be the sum of the stray capacitances C_1 to C_6 . To illustrate the difficulty of obtaining good frequency response, let us assume we are trying to measure oscillations in floating potential V_f with a probe 0.25 mm in diameter and 1 mm long in a plasma of density $n = 10^9 \text{ cm}^{-3}$ and temperature $kT = 0.23 \text{ eV}$. To float the probe, we must have $R_L \gg R_p$, and the frequency response is then given by the time constant $R_p C$. The plasma impedance R_p is the slope of the voltage-current characteristic at V_f and is of the order of 10^6 ohms for the conditions given. The stray capacitances are, typically, $C_1 = 12 \text{ pf}$, $C_2 = 100 \text{ pf}$, $C_3 = 50 \text{ pf}$, $C_4 = 50 \text{ pf}$, $C_5 = 150 \text{ pf}$, $C_6 = 50 \text{ pf}$; thus, $C \approx 400 \text{ pf}$ and $R_p C \approx 4 \times 10^{-4} \text{ sec}$. The response will be down 6 dB at $\omega = \sqrt{3}/R_p C$, or $f = 700 \text{ Hz}$. Even at $n = 10^{10} \text{ cm}^{-3}$, the response will be good to only 7 kHz.

This can be improved by incorporating a transistor amplifier into the probe shaft so that only C_1 , which is unavoidable, remains. However, at $n = 10^9 \text{ cm}^{-3}$, the response is still good only to 20 kHz. For this reason, we have chosen a method employing coaxial probes, described in Sec. II, and capacitance neutralization, described in Sec. III.

II. DESIGN OF PROBES

Figure 2 is a mechanical drawing of a coaxial probe assembly. A 6.4 mm diam stainless steel tube serves as a vacuum jacket and a grounded shield. Another stainless steel tube, insulated from the outer tube by teflon tape, forms a floating inner shield and is connected to the body of a standard BNC fitting. The center pin of this fitting is replaced by the end of a long tungsten rod, which serves as the probe lead. An 0.05 mm diam wire is spotwelded to the other end of the center rod; this is the probe itself. Vacuum seals are made by four small O-rings. The insulator extending into the plasma consists of two coaxial pyrex tubes, 0.25 and 0.10 mm in outside diameter. The outer tube leaves a 2 mm length of the 0.05 mm diam wire exposed as a truly cylindrical probe. The inner tube is recessed about 1 mm and serves to center the probe tip and prevent it from touching any conducting coating that may form on the outer tube. Furthermore, the inner tube is coated with a conducting paint, which is connected to the inner floating shield. Thus the probe is shielded to within 1 mm of the tip, and the overall diameter of the probe is 0.25 mm, which is only $1/4$ of r_{Li} for a K atom at 4 kG. Larger probe tips can, of course, be spotwelded onto the probe tip if desired.

The resistance of the conducting coating is less than 100 ohms, which is adequate for low-frequency observations. For high-frequency electron oscillations, however, the skin depth is too large to provide

adequate shielding. In this case it would be better to use a slightly fatter probe developed by N. Rynn, in which the insulator and inner shield consist of a molybdenum tube sprayed with a thin layer of alumina.

III. FLOATING POTENTIAL FLUCTUATIONS

To overcome the problem of stray capacitance, we have used the method of capacitance neutralization illustrated in Fig. 3. The floating inner shield is connected to the output of a unity-gain amplifier A_1 so that almost zero voltage appears across the capacitance C^* . Thus the capacitive loading of the probe is effectively cancelled. The output of A_1 also goes to an ordinary amplifier A_2 , which drives the long cable from the machine to the oscilloscope or frequency analyzer. For convenience, A_2 is given a gain of 10. Note that the driven shield ensures that the probe picks up only the local oscillations at the probe tip. Provision is made for floating A_1 and A_2 at a bias voltage V_B . The reason for this is shown by the probe characteristic in Fig. 3. Because of the difference in work function between tungsten and alkali metals, the floating potential V_f is normally 4 - 5 volts, so that $eV_f \gg kT_e$. The load resistance R_L then has to be very large if the load line is to cross the probe curve near V_f . If one sets $V_B \approx \bar{V}_f$, however, the origin for the load line will be shifted to \bar{V}_f , and a lower value of input impedance can be tolerated.

The design of a unity-gain amplifier with frequency response to 200 kHz turned out to be very difficult. Note that A_1 has to drive the capacitances C_{1-3} between the inner shield and ground as well as C^* . These capacitances must be reduced to less than 2 pf to meet our requirements, so that the gain of A_1 must be within 1% of unity for all frequencies up to 200 kHz but must not exceed unity at any frequency to avoid oscillation. Such an amplifier has been developed

by E. Grant of the Plasma Physics Laboratory Engineering Division; it is shown in Fig. 4. The input stages consist of two field effect transistors (FET) used as source followers. Following these is a two-transistor complementary-symmetry-pair amplifier providing the unity-gain output. A_2 is another symmetry-pair providing the low-impedance output. To cancel capacitances within the circuit and to avoid oscillation, internal shields and bootstrapping are used. The circuit is dc coupled, but an input capacitor is used to protect the first FET.

This circuit has been tested with an oscillator feeding an input adapter consisting of a low-capacitance $1\text{ M}\Omega$ resistor, representing the probe impedance, shunted by 220 pf , representing C^* . The frequency response is $+1, -6\text{ dB}$ from 10 Hz to 150 kHz for values of C_{1-3} up to 330 pf . Various values of R_L can be switched in without oscillation, so that in principle oscillations in probe current can also be detected with this circuit. However, this first model had too much noise for this application. Figure 5 shows a test of this circuit in an actual plasma. It is seen that the frequency spectrum of V_f fluctuations is in good agreement with the spectrum of J_- (electron saturation current) fluctuations up to 150 kHz if the CNP is used, but not if an ordinary preamplifier is used. A Keithley Type 102B isolation amplifier was also tried, but its noise level was much too high.

IV. SATURATION CURRENT FLUCTUATIONS

To measure J_+ or J_- fluctuations one sets the load resistor R_L (Fig. 1) to a value much smaller than the plasma impedance, given by the slope of the probe characteristic in the saturation regions. The frequency response is then determined by the time constant $R_L C$. One method to reduce $R_L C$ is to build a resistive attenuator inside

the probe shaft and to compensate for the cable capacitance with a variable capacitor. This has the disadvantages (a) that most of the signal power is lost in the attenuator, (b) that the frequency compensation has to be readjusted for different plasma conditions or cable lengths, and (c) that the resistors inside the shaft cannot easily be removed or changed. The availability of low-noise, high-gain, large-bandwidth amplifiers has enabled us to use a much simpler method; namely, simply using a very small R_L . Thus if C_{1-6} (Fig. 1) is 1000 pf and R_L is 1 k Ω , response to 275 kHz is possible. In fact, if R_L is chosen to be the characteristic impedance of the cable (185 Ω for RG 114/U), response to very high frequencies is possible. Of course, the signal becomes very small: for $J_+ = 10^{-7}$ A, $R_L = 1$ k Ω , the signal voltage is only 100 μ V. To amplify this, we have used the Tektronix Type 1A7 plug-in preamplifier, which has 10 μ V/cm sensitivity, 3 μ V rms noise, and 500 kHz bandwidth. It is dc-coupled and has built-in high- and low-pass filters. For J_- oscillations, the currents are usually large enough that a less sensitive preamplifier can be used.

The disadvantage of using J_- as a means of detecting density fluctuations is that the plasma is likely to be disturbed by the large probe currents. Sometimes these currents can excite oscillations, as shown in Fig. 6. The high-frequency peaks in the spectrum of J_- are obviously caused by the probe, because they do not appear in the J_+ spectrum and the frequencies depend on the probe potential.

The use of J_+ for density measurements is less likely to disturb the plasma, but the J_+ spectrum is not the same as the spectrum of density fluctuations. We first noticed this effect when the ratio $\tilde{J}_+ / \langle J_+ \rangle$ appeared to be larger than $\tilde{J}_- / \langle J_- \rangle$, and in fact J_+ was sometimes found to go negative. Figure 7 illustrates the disparity that sometimes occurs between J_- and J_+ spectra, with J_+ showing a preference for high frequencies. We believe that the reason for

the disparity is that at low plasma densities a probe acts partly as a Langmuir probe drawing particle current and partly as an antenna drawing displacement current. Tests with a glass-covered probe have shown that the displacement current can be quite large. We give below a simple one-dimensional treatment of this effect.

Consider a plane probe drawing saturation ion current. The probe current j_p per cm^2 is

$$j_p = j_i + j_d \quad , \quad (1)$$

where j_i is the ion conduction current and j_d the displacement current, given by

$$j_d = \frac{1}{4\pi} \frac{\partial E}{\partial t} \quad , \quad (2)$$

E being the electric field at the probe surface. For $|eV_p/kT| \gg 1$, E can be approximated by using the Child-Langmuir space charge law /1/:

$$|E| \approx 2(\pi n)^{1/2} (2kT e |V_p|)^{1/4} \quad . \quad (3)$$

To obtain this we have given the space-charge-limited current j_i the Bohm value /2/:

$$j_i \approx \frac{1}{2} ne(kT/M)^{1/2} \quad . \quad (4)$$

Taking the time derivative of Eq. (3), indicated by a dot, and using Eq. (2), we find

$$|j_d| = \frac{|E|}{8\pi} \left(\frac{\dot{n}}{n} - \frac{1}{2} \frac{\dot{V}_p}{V_p} \right) \quad . \quad (5)$$

Here we have used the fact that a fluctuation \hat{V} of the plasma potential at the sheath edge is equivalent to $-\hat{V}_p$. For $|\hat{V}| \leq \omega kT/e \ll \omega |V_p|$, the second term in Eq. (5) is much smaller than the first. We can also write Eq. (5) as

$$|j_d| = \dot{C}_s V_p + C_s \dot{V}_p \quad , \quad (6)$$

in which C_s is the sheath capacitance. Thus at frequencies below ω_{pi} , the main contribution to j_d is the change in sheath capacitance due to a change in Debye length when n fluctuates. At frequencies above ω_{pi} , the ions cannot move, C_s is constant, and the probe picks up potential fluctuations.

For low frequencies, we see from Eqs. (3), (4), and (5) that $|j_d/j_i|$ is proportional to $\omega M^{1/2} n^{-1/2} V_p^{1/4}$, explaining why J_+ has more high frequency power than J_- in low-density plasmas. The magnitude of $|j_d/j_i|$ is of order 0.5 for $n = 10^9 \text{ cm}^{-3}$, $f = 500 \text{ kHz}$, and $\tilde{n} / \langle n \rangle \approx 1$.

REFERENCES

- /1/ F. F. Chen, "Electric Probes," in Plasma Diagnostic Techniques,
ed. by R. H. Huddlestone and S. L. Leonard (Academic Press,
New York, 1965), Chap. 4, p. 119, Eq. (10).
- /2/ Ibid., p. 150, Eq. (105).

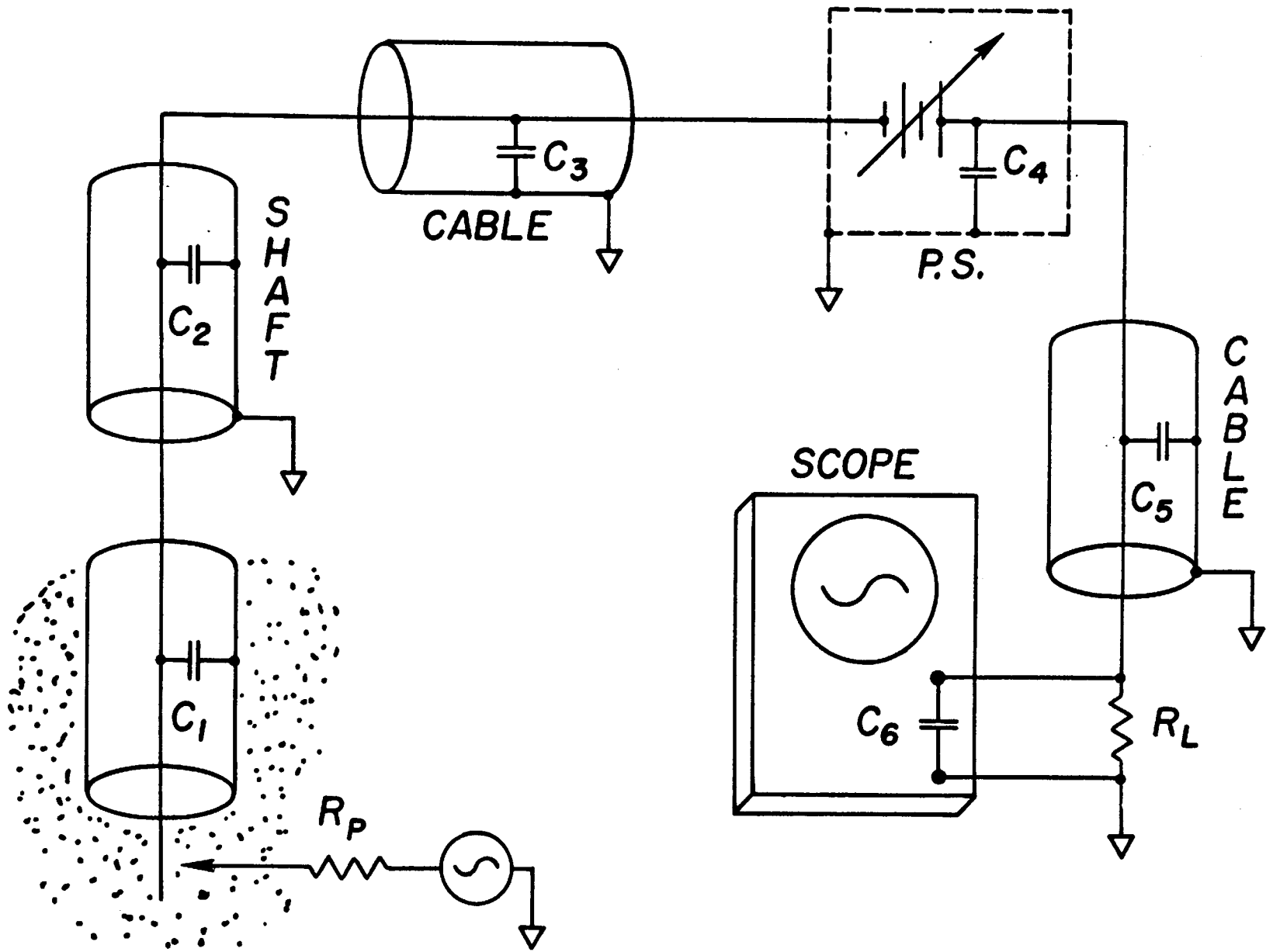


Figure 1

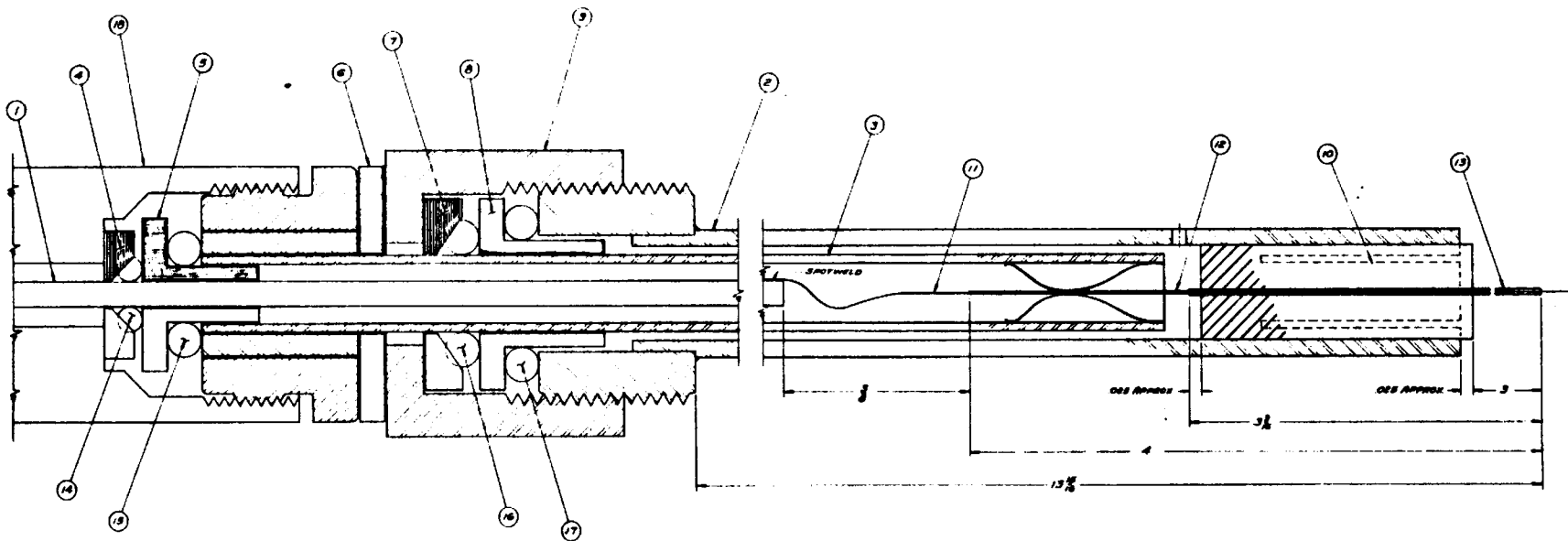


Figure 2

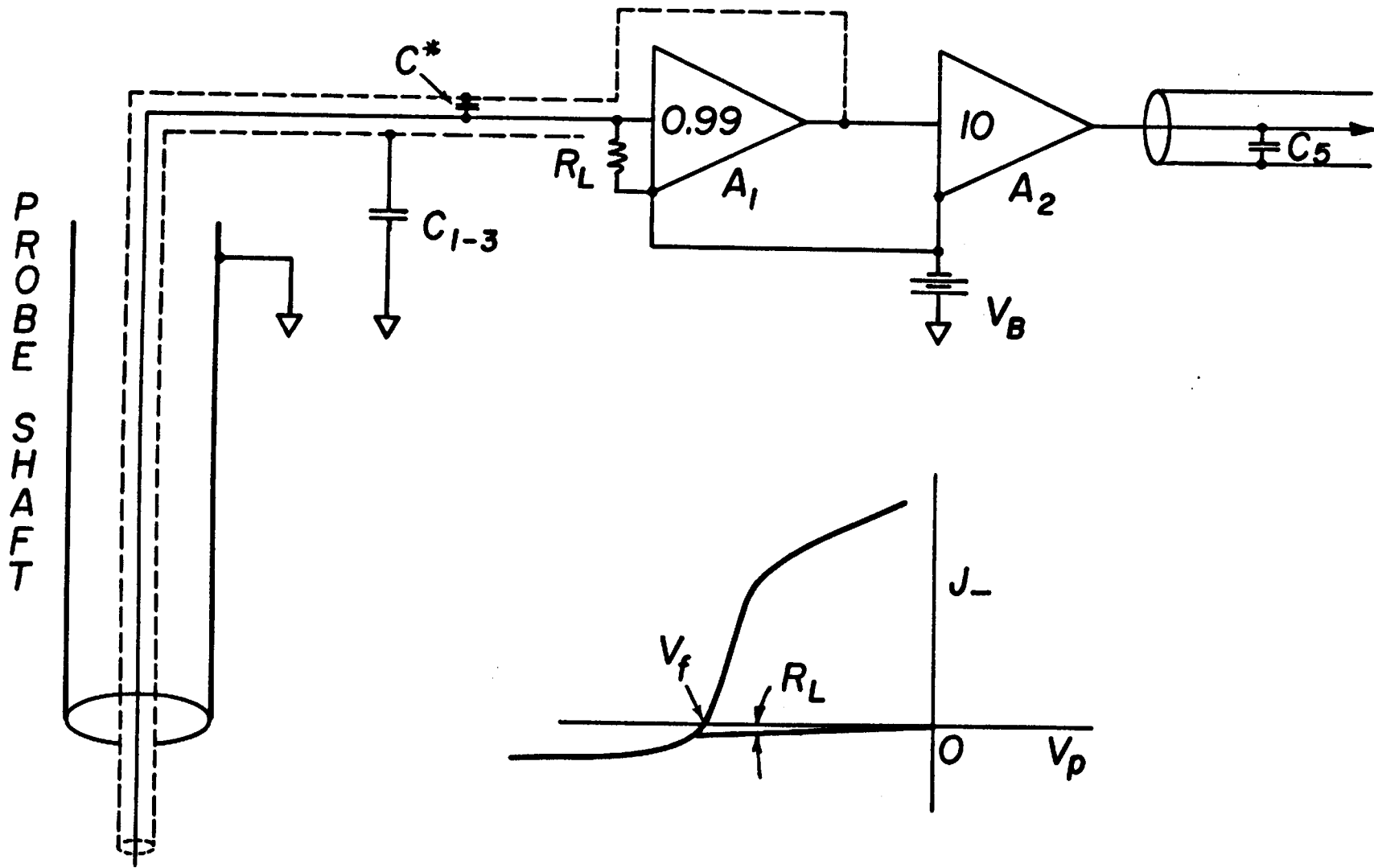
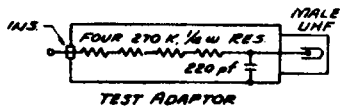
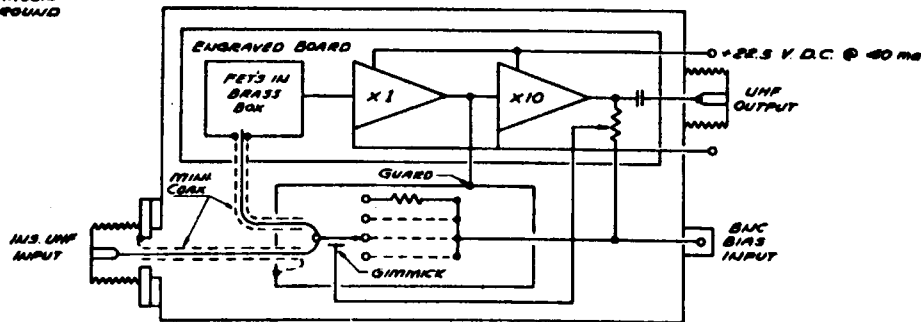
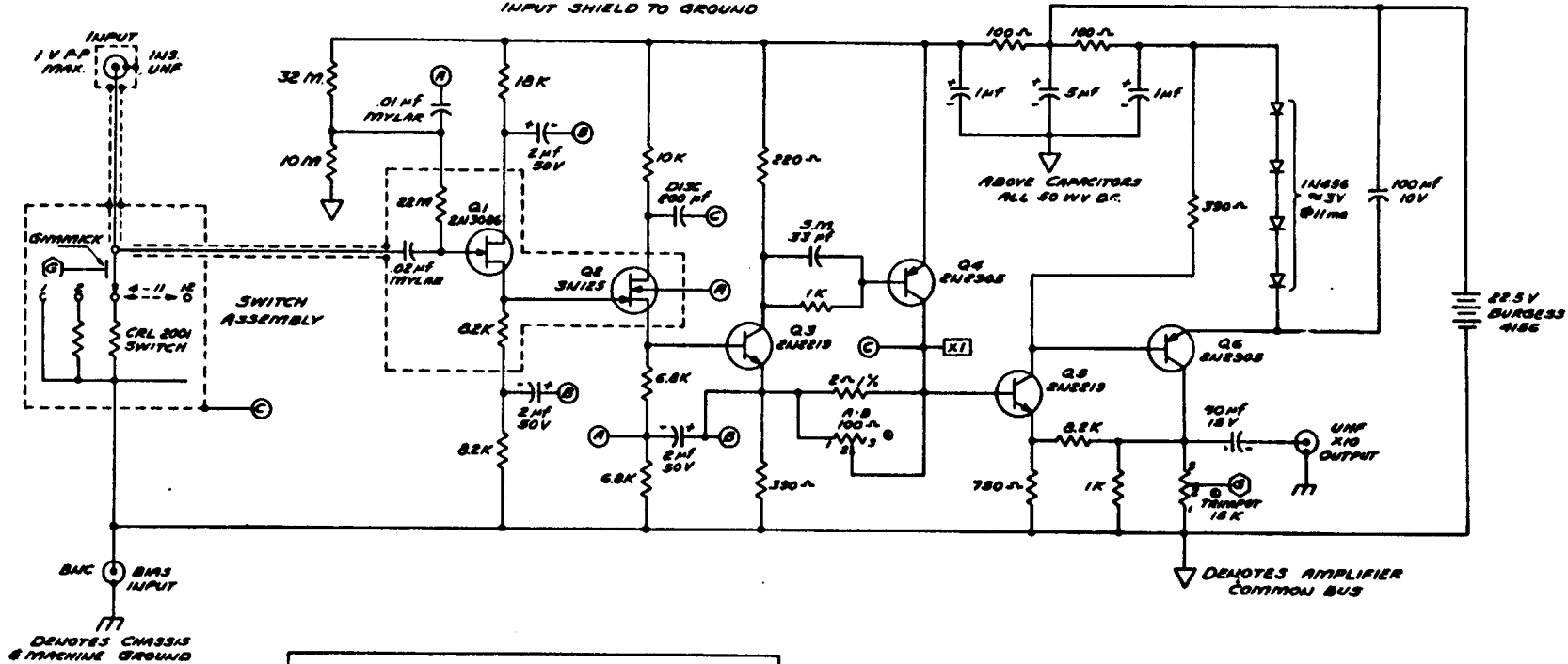


Figure 3



USE TEST ADAPTOR

SW IN = POS.
 $f_1 < 20 \text{ MHz}$
 $f_2 = 150 \text{ KHz} - 6 \text{ dB}$
 CAN DRIVE 330 pF
 INPUT SHIELD TO GROUND



POS. NO.	RESISTANCE
1	0 Ω
2	10 Ω
3	100 Ω
4	1 K
5	10 K
6	100 K
7	200 K
8	300 K
9	1 M
10	2 M
11	5 M
12	∞

Figure 4

PERFORMANCE OF CNP

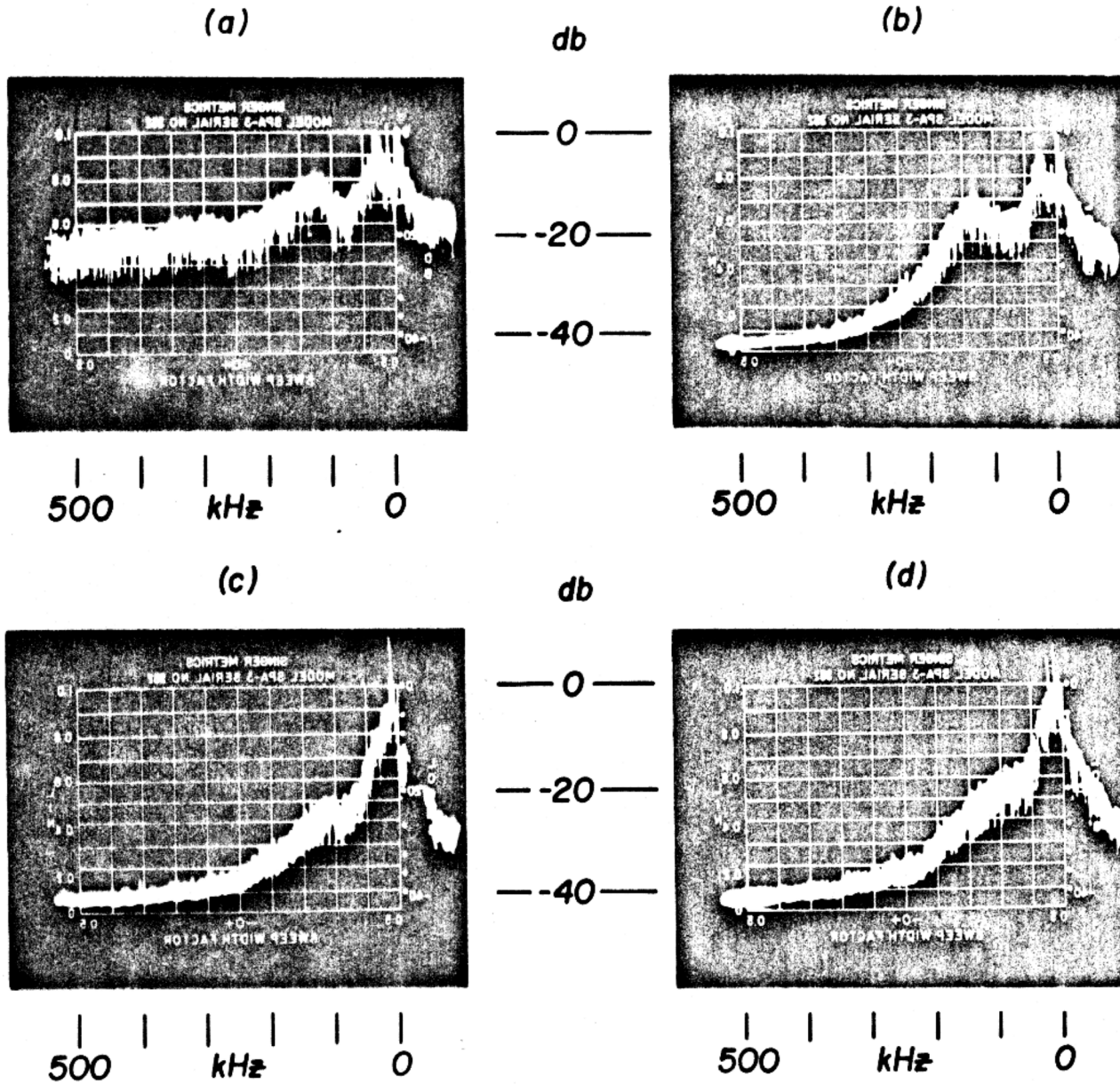
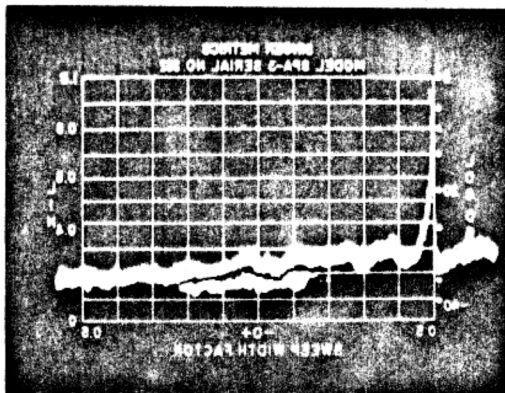


Figure 5

OSCILLATIONS EXCITED BY PROBE

(a) J_+ , $V_p = -8V$

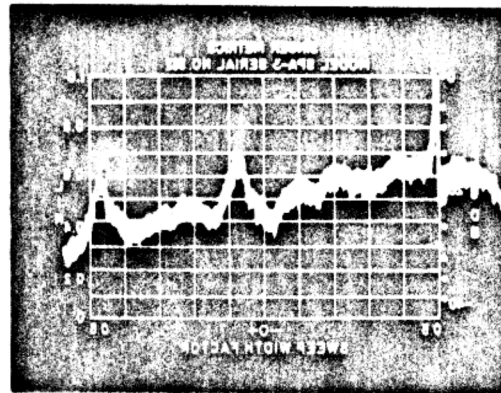


500 kHz 0

(b) J_- , $V_p = 0V$

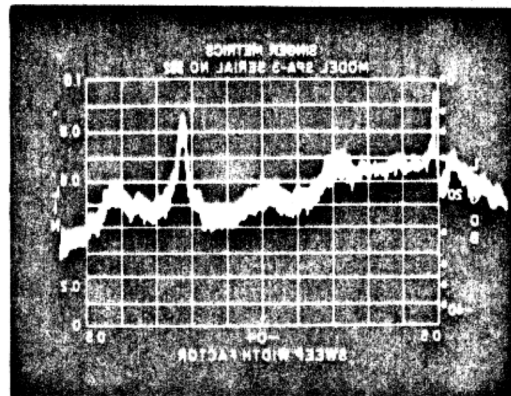
db

0
-20
-40



500 kHz 0

(c) J_- , $V_p = +2V$

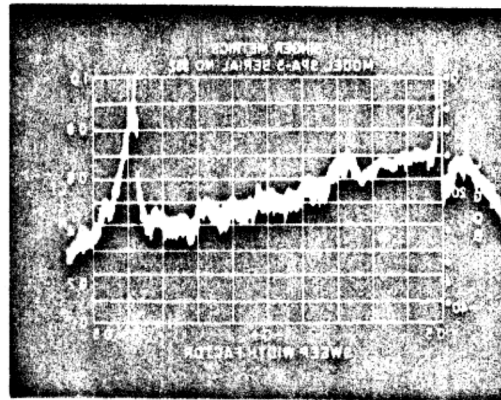


500 kHz 0

(d) J_- , $V_p = +4V$

db

0
-20
-40

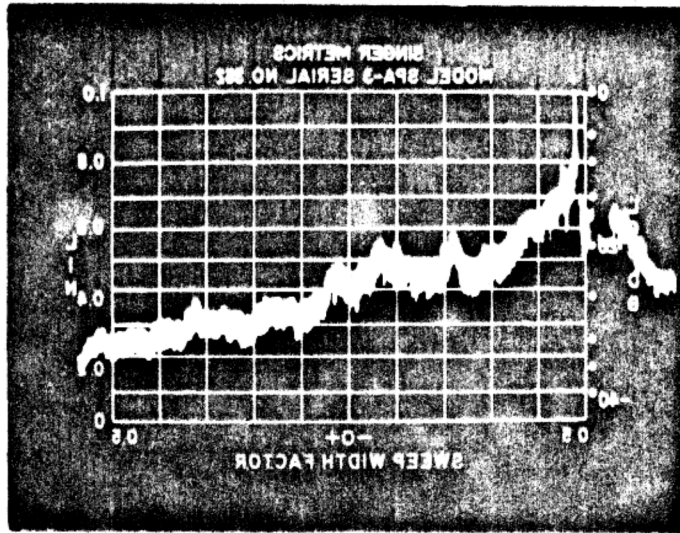


500 kHz 0

Figure 6

COMPARISON OF J_- , J_+ SPECTRA

J_-



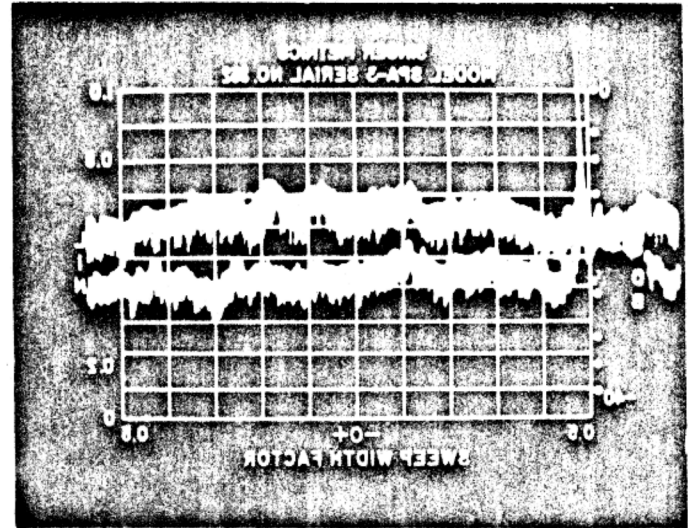
db

— 0 —

-- 20 —

-- 40 —

J_+ 10 X GAIN



500 kHz 0

500 kHz 0

Figure 7